Available online at www.sciencedirect.com
SciVerse ScienceDirect
Procedia Environmental Sciences 17 (2013) 503 – 512
Procedia Environmental Sciences

The 3rd International Conference on Sustainable Future for Human Security
SUSTAIN 2012

Experimental and theoretical model for water desalination by humidification - dehumidification (HDH)

Mohamed S. Mahmoud[a*], Taha E. Farrag[a], Wael A. Mohamed[a]

[a] *Department of Chemical Engineering, Faculty of Engineering, Minia University, Minia City, 61516, Egypt,*

Abstract

This paper aims to provide both experimental and theoretical model for utilization of Fresnel lens in solar water desalination by humidification-dehumidification process. The work was done in two stages. The first stage aimed at investigating the performance of Fresnel lens in heating saline water. Solar energy is considered as a source of heating. For thermodynamic analysis, mass and energy balance equations have been developed for the water heating, humidifier, and other cycle components. The models were solved numerically and validation showed that the model outcomes are 25% higher than the experimental data due to energy losses. The analysis indicates that Fresnel lens collector has good efficiency (70%) in clear days. The influence of ambient conditions and the percent of different types of energy loss, etc., are also analyzed. The second stage was to perform experiments for intensification of fresh water yield from the unit. The experiments were done for both open and close loop of air. The results showed that closed loop system provides higher water production than open loop system..

Keywords: Solar, Water, Desalination, Humidification, Dehumidification

1. Introduction

Restricted resources of fresh water are always considered inadequate in future due to population increase as well as expansion of urban and industrial developments. The current processes for water desalination such as reverse osmosis (RO) process and multistage flashing (MSF) processes can be used to supply the future needs of fresh water; however the energy requirement will be the stumbling block.

* Corresponding author. Tel.: +2-086-236208; fax: +2-086-2346674
E-mail address : m.salah.m@mu.edu.eg

doi:10.1016/j.proenv.2013.02.065

While the world fights to reduce the CO_2 output for future environment, the production of fresh water with current methods ought to increase the CO_2 output. Development and implementation of new technologies for small capacity plants is highly enviable.

Nomenclature

A	Area, m^2 (subscripts: *o*=outer area of steel pipe, *r*= area of radiation heat loss, *tot*= the total area of the air flow, *w*= the area of water drop)
D	Diameter, m (subscripts: *i*= inner diameter of steel pipe, *o*= outer diameter of steel pipe, *p*= water drop diameter)
H	Enthalpy of water, kJ/kg
h_o	Heat transfer coefficient based on outer area of steel pipe, W/m^{2}K
Kc	Mass transfer coefficient, m/s
q_{in}	Thermal flux intensity, W/m^2
q_{in}	Thermal intensity, W
Q_{in}	Heat input, kW
r	The droplet radius, m
T	Temperature, K (subscripts: *air*= temperature of air, *ew*= temperature of water entering steel pipe, *f*= temperature of water exiting the studied steel slice, *i*= temperature at interface, *ow*= temperature of water exiting steel pipe, *so*= outer temperature of steel pipe, *si*= inner temperature of steel pipe, *w in*= temperature of water entering HD unit, *w out*= temperature of water exiting HD unit, *x* = temperature of the bulk of liquid, *y*= temperature of bulk of gas)
V_w	The volume of water drop, m^3
W	Rate of evaporation, kg/s
x	Thickness of the studied steel slice, m
ΔT_{LM}	Logarithmic mean temperature difference, ^{o}C

The HDH process is based on the fact that air can be mixed with important quantities of vapor. The amount of vapor able to be carried by air increases with the temperature; in fact, 1 kg of dry air can carry 0.5 kg of vapor and about 670 kcal when its temperature increases from 30°C to 80°C [1]. When airflow is in contact with salt water, air extracts a certain quantity of vapor at the expense of sensible heat of salt water, provoking cooling. On the other hand, the distilled water is recovered by maintaining humid air at contact with the cooling surface, causing the condensation of a part of vapor mixed with air. Generally the condensation occurs in another exchanger in which salt water is preheated by latent heat recovery. An external heat contribution is thus necessary to compensate for the sensible heat loss. Energy consumption is represented by this heat and by the mechanical energy required for the pumps and the blowers.

Solar water desalination with HDH processes has been proven to be an efficient means of production of fresh water in remote and sunny regions. Numerous solar desalination installations concerned with small and medium production have been developed and studied. Many researchers investigated the HDH desalination processes. Most investigations on the HDH desalination process have focused on productivity and efficiency improvement [1~7]. However, limited studies focused on the enhancement of solar energy utilization for saline water heating before it is introduced to HDH desalination process [8]. Here we propose to use Fresnel lens for saline water heating. The Fresnel lens (FL) is a flat optical solar concentrator; the surface is made up of many small concentric grooves. Each groove is approximated by a flat surface that reflects the curvature at that position of the conventional lens, so each groove behaves like an individual prism. Solar energy concentrated by FL is a cheap and environmentally friendly energy source suitable for many applications such as surface materials treatments. The advantages of the Fresnel installation make it a serious alternative to some conventional techniques used in this field [9].

In this paper, we demonstrate both experiments and mathematical model for utilization of an economical and high efficiency method for solar heating by FL in developing a solar of water desalination by HDH.

2. Methodology

Figure 1 illustrates a schematic diagram of the experimental setup. The FL shown in the insertion of Fig. 1 consists of acrylic sheet with concentric grooves with focal length of 0.85 m. The lens was fixed facing south with a tilt angle of 28^o in summer season, the solar tracking is done manually throughout the daylight. The saline water passes through pipe, its properties is shown in Table 1. The water storage tank is made from steel and sealed by glass wool in order to reduce the heat loss; also it is supplied with electrical heater to adjust the temperature of hot saline water to the desired feed temperature. As indicated in Fig. 1, water pass with a different flow rates once through the heating pipe where it is heated by the focused solar energy. Once the water temperature reaches the desired starting temperature, water is directed to the humidification unit.

The humidification-dehumidification unit consists of galvanized steel cuboids of 0.001m thickness lined with plastic sheet. The air is inserted to the unit by fan with 0.25 m diameter mounted on one face of the tank. The velocity of inlet air is measured by using hot wire anemometer and the average velocity of inlet air can be calculated by

$$u_o = \frac{\int udA}{A_{tot}} \tag{1}$$

The average flow rate was 0.11 m^3/s and average air velocity of 4.5 m/s. The vapor content difference is defined as

$$\Delta H = H_{out} - H_{in} \tag{2}$$

where H_{in}, H_{out} are the inlet outlet humidity of the unit. The humidification efficiency of the unit is given by

$$\eta_{hu} = 100 \times \frac{H_{out} - H_{in}}{H_{sat} - H_{in}} \tag{3}$$

On the opposite face, a condenser is fixed. The fresh water resulting from treatment process is collected through a header channel mounted below the condenser. The rotating disc sprayer is placed inside the unit and 0.2 m in front of the fan to perform the misting of saline water to get droplets with diameter in mm range. The unit has discharge weir for recycling of miscarried water to the storage tank, and is covered by transparent plastic cover to keep the air inside. The initial volume of saline water is 25 l and average experiment duration is 15 min. The exhaust air coming out of the condenser is either recycled (closed loop of air) or expelled away (open loop of air). The concentration of salt was measured by AZ 86555 laboratory bench top meter supplied by AZ Instrument Corp. The temperature of hot feed water and air and the humidity at the inlet and the outlet of each part of the unit and the water and air mass flow rates are measured. The studied parameters include the sprayer rotation speed and the feed water temperature.

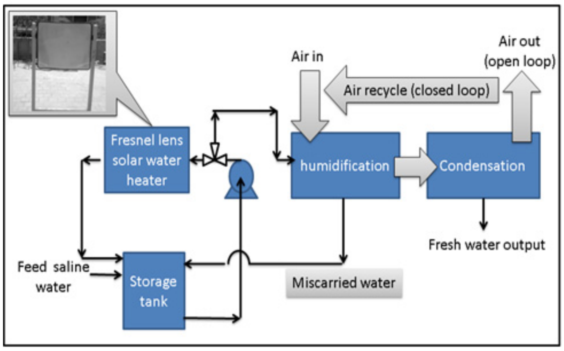

Fig. 1: Setup of the experiment, insertion: Fresnel lens.

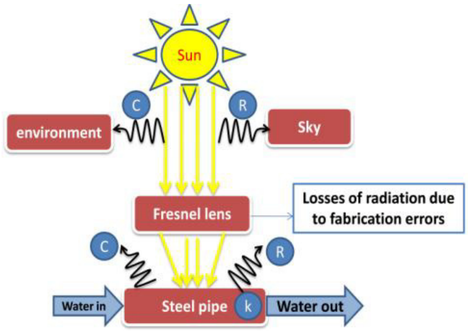

Fig. 2: Thermal resistances and losses of solar radiation

3. Mathematical Model

In the following, we are going to build a mathematical model for the whole system starting from the FL system and ended with the yield of the desalinated water. In order to increase the efficiency of humidification process, heating the feed water is necessary to boost mass transfer and fortify evaporation. The FL solar collector concentrates the incident solar radiation in a spot. If we direct this spot to heat the steel pipe, then the saline water will be heated to the experiment starting temperature. The theoretical prediction of the water temperature coming out from the FL system is calculated with the aid of energy balance around FL heating system. A mathematical model which describes the dynamic energy performance of the Fresnel lens solar collector is first developed. In order to simplify the analysis, some assumptions are made as follows:

(1) It is assumed that the Fresnel lens is not ideal i.e. contain some fabrication errors because it is a commercial grade. Any incident solar radiation on the lens, will suffer from 30~ 40% losses and the reminder solar radiation be concentrated on absorber [10].
(2) The transmittance, reflectance and absorbance of the collector components are considered to take their mean values and do not vary, irrespective of the incident beam direction.
(3) The variation of temperature along the axial direction of the steel pipe collector is neglected.
(4) The thermal properties of component materials are constant and those of air and water are obtained from the thermal properties data [11].
(5) For air–water vapor mixtures. The outlet water from the humidification unit could not be cooled to a temperature lower than the inlet air wet bulb temperature.
(6) The average air velocity in Minia Governorate, Egypt is 4~6 m/s [12]. Relative humidity of inlet air was measured on July 15th to be 30~40% according to the average climate conditions of Minia Governorate, Egypt.
(7) Operation occurs at a constant atmospheric pressure of 101,330 Pa.

Table 1: design parameters of the heating system and HD unit

Experimental part	property	value
Fresnel lens	Length × Width	50 ×70 cm
	Focal length	85 cm
	Material of construction	Acrylic
Heating pipe	Length	20 cm
	Nominal size	¾ in
	Schedule no.	40
	Outside diameter	1.050 in
	Inside diameter	0.824 in
	Wall thickness	0.113 in
	Material of construction	Steel
Humidification unit	Length × Width ×Height	80×50×50 cm
	Material of construction	Galvanized steel
Condenser unit	Length × Width ×Height	30×60×30 cm
	Material of construction	Copper

Equation (4) represents the relation between the sun and earth geometry and their relation with the solar intensity concentration, where F is the length power, $F = f/d_{\text{lens}}$, f is the focal length (m), d_{lens} is the diameter of the FL (m), L is the length from sun to earth (m), r_{sun} is the radius of sun (m), I_{spot} is the spot intensity (W/m^2), and I_o is the incidence solar intensity.

$$F^2 I_{spot} = \left(\frac{L}{r_{sun}}\right)^2 I_o \tag{4}$$

The energy flow and thermal resistance among the elements of the collector and the surroundings are described in the thermal network drawn schematically in Fig. 2. Here, K represents the conductive thermal resistance, C represents the convection thermal resistance and R represents the radiation thermal resistance. Based on the aforementioned assumption, the following dynamic energy balance formulas for every component are derived.

Steel pipe:

$$(m_{air} c_{p_{air}}) \frac{dT_{so}}{dt} = I_{spot} + \frac{T_{air} - T_{so}}{R_c} + \frac{T_{air} - T_{so}}{R_R} + \frac{T_{si} - T_{so}}{R_k} \tag{5}$$

where the incident beam solar radiations at the spot includes the concentrated solar energy absorbed by steel pipe and the reflected solar energy by the pipe with selective coating, the actual energy obtained at the spot is given by :

$$I_{spot\,actual} = I_{spot} \eta_F \alpha_F A_F \tag{6}$$

The thermal resistance in energy balance formulas can be calculated via the expressions in Table 2. The corresponding thermal resistances are illustrated in Fig. 2. The input parameters for the model are list in Table 3.

The temperature of water exiting from steel pipe could be calculated based on energy balance through a small slice of steel pipe. The following assumptions should be considered:

1- Constant heat flux model prevails.
2- Physical properties remain constant and calculated at mean temperature
3- Change in kinetic and potential energy are negligible

Table 2: Thermal resistances and applied equations/correlations in the model

Thermal resistance	Applied equation/ correlation	Equation no.	Ref.
$R_k = (r_o - r_i)/k_{steel} A_{lm}$	$q_{cond} = kAdT/dz$	(14)	[13]
$R_{c-air} = 1/h_o A_o$	$q_{conv} = h_o A\Delta T$ $Nu = hd_o/k = 0.26\,\mathrm{Re}^{0.6}\,\mathrm{Pr}^{0.2}$	(15) (16)	[13]
R_r	$q_{Rad} = A_r \varepsilon\sigma T^4$	(17)	[13]

Table 3: Parameters of the Fresnel lens solar collector and the steel pipe

Symbol	Meaning	Value	Unit	Ref.
u_{air}	Velocity of air	5	m/s	[12]
ρ_{air}	Density of air	1.113	Kg/m^3	[11]
μ_{air}	Viscosity of air	1.93×10^{-5}	Pa.s	[11]
k_{air}	Thermal conductivity of air	0.025	W/mK	[13]
$c_{p\ air}$	Air specific heat	1004.8	J/kgK	[13]
$\rho_{-water\ at 50^oC}$	Density of water	988	Kg/m^3	[14]
$c_{p-\ water\ at 50^oC}$	Water specific heat	4183	J/kgK	[14]
k_{steel}	Thermal conductivity of steel	45	W/mK	[14]
f	Focus length	0.5	m	-
L	Length from sun to earth	1.5×10^{11}	m	-
R_{sun}	Radius of sun	6.96×10^{8}	m	-
I_o	The incidence solar intensity	800	W/m^2	[8]
η_F	Fresnel lens efficiency	0.6	-	[15]
α_F	Factor of losses due to manufacturing errors	0.8	-	[10]
ε	Emissivity of bodies other than black	1	-	[11]
σ	Constant	5.676×10^{-8}	W/m^2K^4	[11]
$D_{Air-H2O}$	Diffusivity of air relative to water	0.288×10^{-4}	m^2/s	[11]
$P^*_{H2O\ at\ 80^oC}$	Water vapor pressure	47.34	kPa	[11]

The inventory rate equation for energy balance through small slice of steel pipe becomes

$$q_{in} - h_{w-in} - (h_{w-in} + \frac{d}{dx}(h_{w-in})dx) = \frac{dh}{dt} \tag{7}$$

At steady state the rate equation for energy reduces to

$$q_{in} = \frac{d}{dx}(h_{w-in})dx = \frac{d}{dx}(\dot{m}\, c_{p-water} dT_f)dx \tag{8}$$

Assuming that the incident energy from solar radiation is homogeneously distributed over the surface of the small slice of steel pipe:

$$q_{in} = q_{in}^{`} A = q_{in}^{`} \pi d_o dx \tag{9}$$

Substitute of (9) in (8) gives:

$$q_{in}^{`}\pi d_o dx = \frac{d}{dx}(\dot{m} c_{p-water} dT_f)dx \tag{10}$$

By rearrangement

$$q_{in}^{`} = \frac{mc_{p-water}}{\pi d_o}\frac{dT_f}{dx} = \frac{q_{in}^{`}\pi d_o}{mc_{p-water}} \tag{11}$$

by integration of (11)

$$T_f(x) = \frac{q_{in}^{`}\pi d_o}{mc_{p-water}}x + c \tag{12}$$

The initial conditions is ($x = 0 \quad T_f = T_{ew}$)

$$T_f(x) = \frac{q_{in}^{`}\pi d_o}{mc_{p-water}}x + T_{ew} \tag{13}$$

Subsequently, we studied air humidification operation in terms of mass transfer for air flow across water drops. The rate of evaporation of water from solution depends on the geometry of contact between water and air. In the case of spherical water droplets sprayed in air stream, the rate of evaporation depends on the particle diameter as follows [11]

$$K_c^{`} = \frac{2D_{AB}}{d_p} \tag{14}$$

It is notable that decreasing particle diameter will increase the mass transfer coefficient and accordingly the rate of evaporation will increase. Therefore, the recommended way for efficient evaporation is to produce very fine droplets, which fly very fast through dry air. We can estimate the condition by boundary layer theory. The rate of mass transfer (N_A) for flow of air across water droplets is obtained by:

$$N_A = K_c(c_{A1} - c_{A2}) = K_G(p_{A1} - p_{A2}) \tag{15}$$

The mass transfer coefficient *(K_c)* can be obtained from the following formula for Reynolds number (*Re*) range (1-480000) and Schmidt number (*Sc*) of (0.6-2.7) [11]:

$$Sh = 2 + 0.552\,\mathrm{Re}^{0.53}\,Sc^{0.33} \qquad (16$$

We can compute the evaporation rate (W) by using N_A

$$W = N_A M_{wt}\frac{A_w}{V_w \rho_w} = N_A M_{wt}\frac{4\pi r^2}{4/3\pi r^3\ \rho_w} \tag{17}$$

4. Results and discussion

4.1. Solar water heating

The spot intensity is calculated from Eq. (4) to be 22.4×10^3 kW/m^2, then Eq. (6) was used to calculate the incident solar power as following: for spot of 2 cm diameter (3.14×10^{-4} m^2), and if we consider 60% FL efficiency and 20% losses per FL area (in this experiment the FL area was 0.35 m^2) due to fabrication errors, the incident power will be 1.18 kW. Furthermore, by considering the thermal resistance from Table 2, the heat loss due to convection is calculated to be 915 W. Also, the energy loss due to radiation is calculated based on spot area radiation. Then the power loss due to radiation is 17.9 W. Substituting in Eq. (5), taking into consideration steady state condition, the energy available for conduction to water will be 248.9 W.

The theoretical prediction of water temperature exiting from the steel pipe is obtained from Eq. (7-13). Also the relation between inlet water flow rate and the average emerging water temperature is depicted in Fig. 3, where both theoretical and experimental results are represented. It can be noticed that there is divergence between theoretical and experimental exit water temperature at lower water flow rates. This is mainly attributed to the assumption that all energy conducted through the steel pipe is perfectly used to heat water, yet the experimental results showed that there are losses in energy at higher flow rates. Figure 3 also suggests that in order to heat water to the desired temperature for HDH experiment, it is necessary to use electric heater. However, the solar water heating could be further improved by increasing the area of solar water heating system [16] or utilization of more efficient scheme to heat water such as linear Fresnel lens [8].

4.2. Air humidification- dehumidification

Equations (14-17) predict the evaporation rate corresponding to average water drop diameter $\overline{D}_p$, and plot of the calculated values of evaporation rate against $\overline{D}_p$, is depected in Fig. 4. It can be noticed that water drop diameter has significant effect on the rate of evaporation; furthermore, the effect of air speed on the rate of water evaporation is mild. This figure also indicates that if water droplet of 1 mm radius flies with speed of at least 5 m/s, it completely evaporates within 1 second. The water spraying is thus crucial for enhancement of evaporation rate. To verify this effect we propose to use rotary disc sprayer. A dimensional equation for the volume-surface mean diameter $\overline{D}_p$ of the drop from a disc sprayer [14]:

$$\overline{D_p} = 12.2\times10^4 r\left(\frac{\Gamma}{\rho_w \pi r^2}\right)^{0.6}\left(\frac{\mu}{\Gamma}\right)^{0.2}\left(\frac{\sigma \rho_w L_p}{\Gamma^2}\right)^{0.1} \tag{18}$$

Figure 5 shows a plot of the relation between sprayer rotation speed and the calculated value of $\overline{D}_p$. It can be noticed that the mean diameter of water droplet decrease by 42% as the rotation speed tirples and this will considerabley affect the rate of humidification leading to enhancement of the production yield.

Theoretically, the more dominant parameter is inlet water temperature; its effect on evaporation rate is pronounced. To verify its importance, experiments was done to obtain fresh water yield at different inlet water temperature. Figure 6 shows both open loop and closed loop experiments. It can be noticed that at inlet water temperature of 90 ^{o}C, the maximum attainable water flow rate was 27 L/h/ m^3 of feed saline water for open loop while it reaches 40.8 L/h/m^3 for closed loop. On the other hand, the yield per solar collector area could also be calculated from data shown in Fig. 6. The calculation is based on the theoretical predictions of FL performance discussed previously. The maximum yield of 60 L/d/m^2 of FL collector for open loop and 112 L/d/m^2 for closed loop are predicted in comparison with an ultimate published data of (12 ~ 35.7) L/d/m^2 of solar collector [4, 17].

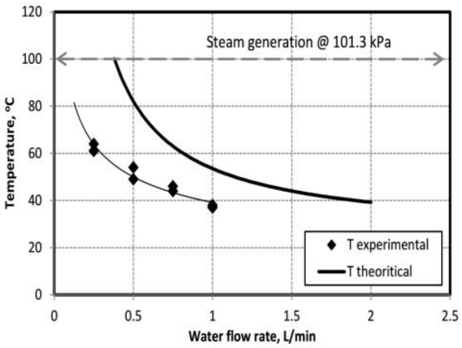

Fig. 3: The relation between inlet water flow rate and water temperature; the experiment was done from 12:00 to 15:00 on July 12, 2011

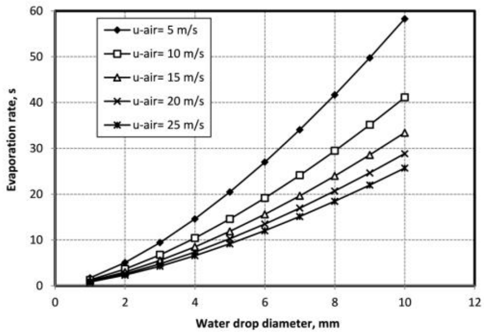

Fig. 4: The relation between drop water diameter and the evaporation rate

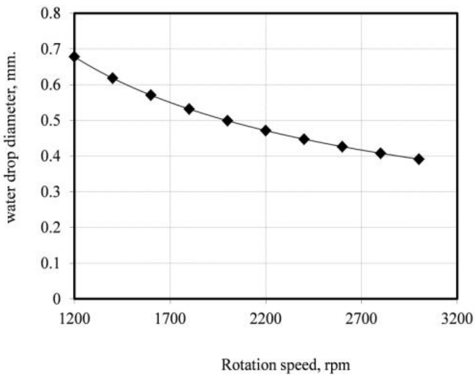

Fig. 5: Theoretical prediction of average water drop diameter at different rotational speed

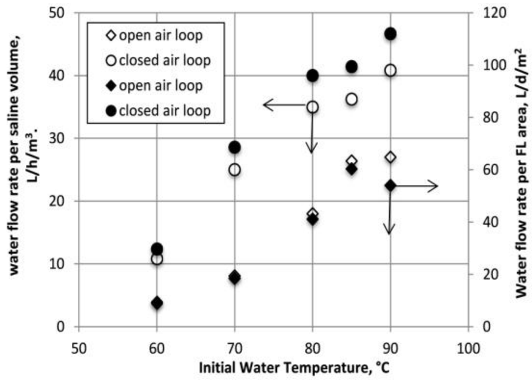

Fig. 6: Effect of inlet water temperature on the freshwater yield at sprayer speed of 2200 rpm

Furthermore, it is noticeable that the temperature of miscarried water is sufficiently high to be further used. In this experiment we recycled this water to be reused, however this design could be further enhanced by introducing miscarried water to second humidification stage to increase the fresh water yield.

5. Conclusion

To conclude, we have presented a comparison study of the possibilities of the use of Fresnel lenses in the development of water desalination system by humidification-dehumidification technique. The main results for this paper can be short noted as follows

- The mathematical modeling for water heated by Fresnel lens showed that the theoretical yield was not accomplished due to energy losses; also the experiment showed that hot water yield depends on water flow rate.
- Mathematical modeling of water evaporation sowed that we could enhance the rate of

evaporation by decreasing water drop diameter, which could be attained by high rotation speed sprayer.

- At inlet water temperature of 90 ^{o}C, the water flow rate were 27 and 40.8 L/h/ m^3 of feed saline water for open and closed loop systems respectively, The temperature of miscarried water is high enough to be introduced to a second stage of the humidification system.

Acknowledgements

The Misr El Kheir Foundation is gratefully acknowledged for the support of this work under grant agreement between Misr El Kheir foundation and Minia University-Faculty of Engineering.

References

[1] K. Bourouni, M.T. Chaibi, L. Tadrist, Water desalination by humidification and dehumidification of air: State of the art, *Desalination*, 2001; **137:** 167–176.

[2] M.F.A. Goosen, S.S. Sablani,W.H. Shayya, C. Paton, H. Al-Hinai, Thermodynamic and Economic Considerations in Solar Desalination, *Desalination*, 2000; **129**: 63–89.

[3] S. Farsad, A. Behzadmehr, Analysis of a solar desalination unit with humidification–dehumidification cycle using DoE method, *Desalination*, 2011; **278**: 70–76.

[4] Said Al-Hallaj, M.M. Farid and A.R. Tamimi, Solar desalination with a humidification-dehumidification cycle: performance of the unit, *Desalination*,1998; **120**: 273–280.

[5] M.M. Farid, N.K. Nawayseh, S. Al-Hallaj and A.R. Tamimi, Solar desalination with humidification dehumidification process: Studies of heat and mass transfer, *Proceedings of Conference: SOLAR 95, Hobart, Tasmania*, 1995; 293–306.

[6] Narayan GP, Ronan K. McGovern a, Syed M. Zubair b, John H. Lienhard V, High-temperature-steam-driven, varied-pressure, humidification-dehumidification system coupled with reverse osmosis for energy- efficient seawater desalination, *Energy*, 2012; **37**: 482-493

[7] Amara MB, Houcine I, Guizani A, Mfialej M., Experimental study of a multiple-effect humidification solar desalination technique, *Desalination*,2004; **170**: 209–221.

[8] H. Zhai, Y.J. Dai *, J.Y. Wu, R.Z. Wang, L.Y. Zhang, Experimental investigation and analysis on a concentrating solar collector using linear Fresnel lens, *Energy Convers. Manage* 2010; **51**: 48–55

[9] CRISTINA SIERRA, ALFONSO J. VA´ ZQUEZ, High solar energy concentration with a Fresnel lens, *J. Mater. Sci*., 2005; **40**: 1339 – 1343.

[10] T. Yabe, T. Ohkubo , S. Uchida, K. Yoshida, B. Bagheri, T. Funatsu, A. Mabuti, A. Oyama,K. Nakagawa, T. Oishi, K. Daito, M. Nakatsuka, M. Yoshida, S. Motokoshi, Y. Sato, C. Baasandash ,N. Nakayama and Y. Okamoto, Experimental Study of Solar Pumped Laser for Magnesium- Hydrogen Energy Cycle, *5th international conference on inertial fusion science and applications Japan*, 2007; 9-14

[11] Christie J. Geankoplis, *Transport processes and unit operation*, Prentice-Hall International Inc., 3rd Edition 1993, pp 236-239

[12] Mortensen, N.G., J.C. Hansen, J. Badger, B.H. Jørgensen, C.B. Hasager, Uwe S. Paulsen, Ole F. Hansen, Karen Enevoldsen, L. Georgy Youssef, U. Said Said, A. Abd El-Salam Moussa, M. Akmal Mahmoud, A. El Sayed Yousef, A. Mahmoud Awad, M. Abd-El Raheem Ahmed, M. A.M. Sayed, M. Hussein Korany, M. Abd- El Baky Tarad, Wind Atlas for Egypt: Measurements, micro- and mesoscale modeling, *Proceedings of the 2006 European Wind Energy Conference and Exhibition, Athens, Greece*, 2006.

[13] J, M. Coulson and J. F. Richardson, *Chemical Engineering Vol 1*, Butterworth Heinemann, 6th Edition 1999, pp 426-428

[14] McCabe, W. L., Smith, J. C., and Harriott, P., *Unit operation of chemical engineering*, McGraw- Hill, New York, 5th Edition 1993, pp 801-803

[15] Reflexite Corporation, Optical design using Fresnel Lenses, http://www.reflexite.com/energy/us/en/, retrieved April 2011.

[16] Joshua FOLARANMI, Design, Construction and Testing of a Parabolic Solar Steam Generator, *Leonardo Electronic J. of Practices & Technologies*,2009; **14**, 115-133

[17] L. Rizzuti et al. (eds.), *Solar Desalination for the 21st Century*, Springer, 2007, 215–225.